Original Paper

Eletrônica de Potência
Open Journal of Power Electronics

Received April 30, 2025; accepted October 20, 2025; Date of publication November 12, 2025.
The review of this paper was arranged by Associate Editor Filipe P. Scalcon and Editor-in-Chief Heverton A. Pereira.

Digital Object Identifier http://doi.org/10.18618/REP.e202557

Development and Experimental Validation of a Field-Oriented Control Voltage Source Inverter for Formula Student Electric Vehicles

Lucas P. da Silva[1,*], Gierri Waltrich[2], Daniel J. Regner[2], Tiago L. F. da C. Pinto[2]

[1]Federal University of Santa Catarina (UFSC), Electrical Engineering Department, Florianópolis, SC, Brazil
[2]Federal University of Santa Catarina (UFSC), Mechanical Engineering Department, Florianópolis, SC, Brazil.

e-mail: lucaspaiva.luc@gmail.com*; gierri@labmetro.ufsc.br; daniel.regner@labmetro.ufsc.br; tiago.pinto@ufsc.br.
*Corresponding author.

ABSTRACT This paper presents the development and validation of a high-reliability three-phase voltage source inverter, designed with field-oriented control (FOC) and space vector modulation (SVM) techniques for use in a Formula Student electric vehicle. Emphasis was placed on achieving efficient power conversion, robust control under variable conditions, and seamless integration with the vehicle's high-voltage and telemetry systems. The inverter was initially validated through Hardware-in-the-Loop (HIL) simulations, followed by bench testing to refine control loop performance, sensor feedback conditioning, and fault protection strategies. Real-world operation during the 2024 Formula SAE Brazil competition demonstrated the inverter's effectiveness, achieving consistent performance, energy efficiency, and thermal stability under dynamic racing conditions. The system's design and validation methodologies contributed directly to competitive success, with the inverter achieving the highest evaluation score in the powertrain category. These results confirm the inverter's robustness, efficiency, and suitability for high-demand electric drive applications, offering a strong foundation for future advancements in vehicular power electronics systems.

KEYWORDS Electric drive systems, Electric vehicles, Field-oriented control, Inverter design, Power electronics.

I. INTRODUCTION

In recent years, the global transition toward electric vehicles (EVs) has accelerated, positioning them as a key solution for sustainable and environmentally conscious transportation. Formula Student, an international engineering competition centered on designing and building high-performance race cars, has embraced this shift through its electric vehicle category. For participating teams, developing an efficient and reliable powertrain is essential, particularly given the resource constraints and evolving technical landscape they face.

This paper builds upon the author's previous work [1], expanding the original inverter design with new experimental validations and performance results. The Formula Student application, shown in Fig. 1, serves as the basis for the development of a three-phase automotive inverter using field-oriented control (FOC) and space vector modulation (SVM). The project addresses engineering and operational challenges unique to competitive electric vehicles.

Initially validated through hardware-in-the-loop (HIL) simulation [2], the inverter was subsequently refined through real-world testing, leading to improvements in reliability, thermal performance, and overall system behavior. Implementation in the vehicle revealed practical challenges and offered valuable insights that enhanced the final design.

FIGURE 1. Ampera Racing Formula Student electric vehicle.

This project also marked a significant milestone: the first successfully implemented inverter by a Brazilian Formula Student Electric team. Strong results in both design and competition performance demonstrated the system's robustness and adaptability under real-world conditions.

The development of custom traction inverters is a recurring challenge in Formula Student, with teams choosing different design priorities and technologies. For example,

Wisconsin Racing reported a compact 120 kW quad inverter targeting high power density and packaging efficiency for a four-motor architecture [3]. Closer to the aims of this paper, Stella *et al.* demonstrated a Formula SAE SiC inverter with online junction-temperature estimation for all MOSFETs, highlighting the relevance of device-temperature awareness in student-built drives [4]. Beyond student projects, recent research prototypes set quantitative benchmarks for power density and thermal robustness in traction inverters: Zhang *et al.* presented a 100 kW SiC inverter achieving $\sim$34 kW/L with operation at 105 °C ambient [5], while Su *et al.* introduced a segmented package architecture exceeding 100 kW/L in less than one liter of volume [6]. At elevated ambient temperatures, Wrzecionko *et al.* showed how SiC devices and targeted thermal management enable air-cooled automotive inverters at 120 °C ambient [7].

On the control side, the paper adopts standard techniques that we reference explicitly for completeness. Field-oriented control (FOC) remains the canonical framework for high-performance AC drives, tracing back to Blaschke's formulation of decoupled torque/flux control [8]. For PWM generation, the relationship between carrier-based modulation and space-vector PWM (SVPWM) is well established and guides our implementation choices [9]. These references ground the controller architecture used here and connect the present design to prior art on thermal/power-density targets and established control practice.

This work presents a cost-effective and reliable inverter based on conventional IGBTs for an AC Induction Motor. It is validated through a systematic design approach and extensive on-vehicle testing. The results demonstrate strong performance and thermal stability under dynamic, real-world conditions, contributing a practical solution for teams facing similar technical and budgetary constraints.

II. FORMULA STUDENT

Formula Student is an international engineering competition where university teams design, build, and compete with electric and autonomous formula-style vehicles. Teams undergo rigorous evaluations through static events—including Design, Cost, and Business Plan presentations—and dynamic events designed to test vehicle performance under realistic conditions.

Static events emphasize engineering excellence, with the Design Event focusing particularly on technical innovation, system integration, and engineering justification. Key components evaluated include the powertrain, chassis, suspension, and control systems.

Dynamic events are critical for validating real-world vehicle performance:

- **Acceleration:** Evaluates the drivetrain's power delivery over a 75-meter sprint.
- **Skidpad:** Measures lateral grip and steady-state cornering balance.
- **Autocross:** Assesses agility and dynamic handling in a short, technical circuit.
- **Endurance:** A 22-kilometer race evaluating reliability, thermal management, and efficiency.
- **Efficiency:** Rewards minimal energy consumption during the Endurance event.

Robust and reliable power electronics significantly impact these outcomes. According to Formula SAE Electric regulations, the accumulator voltage must not exceed 600 V DC, with a maximum power draw of 80 kW. Low-voltage (LV) systems typically operate at 12 V. Essential safety systems include pre-charge and discharge circuits, a Tractive System Active Light (TSAL), and an Isolation Monitoring Device (IMD), ensuring operational safety under all scenarios.

III. THEORETICAL BACKGROUND

To achieve precise and efficient control of electric motors in high-performance applications, such as a Formula Student Electric Vehicle, the selection and understanding of advanced control and modulation strategies are critical. This section outlines the fundamental theoretical principles and methodologies underpinning the chosen techniques for the developed voltage source inverter, ensuring high performance, dynamic response, and reliable operation under the demanding conditions of competitive electric vehicles [8]–[10].

A. Field-Oriented Control (FOC)

Field-Oriented Control (FOC), also known as vector control, is a sophisticated control technique for AC electric motors, including Asynchronous Induction Motors (ACIMs), that allows for the independent control of the magnetic flux and torque-producing components of the stator current [8], [11]. This method effectively decouples these two orthogonal components, mirroring the precise control characteristics typically found in separately excited DC motors. For ACIMs, FOC involves estimating the rotor flux position to orient the stator current vector, thereby enabling highly dynamic and precise torque regulation across a wide speed range [11]. This level of precise control is crucial for high-performance applications demanding rapid acceleration and deceleration, such as a Formula Student vehicle, where immediate and accurate torque delivery directly impacts vehicle performance, driver control, and overall energy efficiency during dynamic maneuvers. While FOC is a well-established technique, its application in custom-built Formula Student powertrains offers clear performance advantages over simpler, scalar control methods [11]. The superior dynamic performance and efficiency offered by FOC are critical for optimizing the limited battery energy and meeting the stringent performance requirements of a competitive electric vehicle, making it an indispensable choice for achieving the desired control fidelity and driving experience.

B. Space Vector Modulation (SVM)

Space Vector Modulation (SVM) is a widely adopted Pulse Width Modulation (PWM) technique used in three-phase voltage source inverters to generate the desired AC voltage waveform [9], [12]. Compared to traditional sinusoidal PWM, SVM offers several significant advantages crucial for high-performance applications like electric vehicles. It maximizes the inverter's output voltage utilization (reaching approximately 15% higher DC bus utilization than SPWM), reduces total harmonic distortion (THD) in the output current, and optimizes switching losses by minimizing the number of switching transitions per fundamental cycle [9], [12]. These benefits directly contribute to higher overall system efficiency, reduced motor heating, and smoother torque delivery, all of which are paramount for the energy constraints and performance requirements of a Formula Student Electric Vehicle. The selection of SVM, despite its widespread use, is critical in this application due to its inherent advantages in maximizing inverter output voltage and minimizing harmonic content compared to simpler PWM schemes. These quantitative benefits directly translate to improved motor performance and reduced system losses, contributing to the competitive edge required in Formula Student environments.

C. Hardware-in-the-Loop (HIL)

Hardware-in-the-Loop (HIL) simulation is an indispensable methodology for the rigorous development, testing, and validation of complex embedded control systems, particularly in automotive and power electronics applications [10]. This technique involves connecting the actual control hardware (in this case, the inverter's microcontroller and its firmware) to a real-time simulation model of the controlled plant (e.g., the electric motor, battery, and vehicle dynamics). HIL allows for comprehensive testing of the control algorithms, protection strategies, and communication interfaces under a wide range of operational conditions, including fault scenarios, that would be difficult, costly, or unsafe to replicate on a physical prototype. For the development of an inverter for a Formula Student vehicle, HIL simulation provides a cost-effective, repeatable, and safe environment to refine the control strategies, debug firmware, and assess system robustness before extensive physical prototyping and vehicle-level integration. In line with best practice for electric-drive development, this work uses a staged HIL $\rightarrow$ bench $\rightarrow$ on-vehicle workflow to accelerate calibration while maintaining correlation to measured behavior [13].

IV. METHODOLOGY

Following the staged workflow introduced in Section III, the inverter development and validation process was organized into three main phases.

1) **Hardware Design and Implementation:** Development of the inverter control and power electronics subsystems, including sensing, gate driving, and protection circuits based on the TMS320F28069M microcontroller.
2) **Hardware-in-the-Loop (HIL) Validation:** Control algorithms and safety logic were tested using a Typhoon HIL real-time emulation of the motor–inverter system. This stage validated control-loop behavior, CAN communication, and fault-handling before powering the actual hardware.
3) **Experimental Validation:** Bench and vehicle-level experiments verified inverter performance under operational conditions, assessing current regulation, torque response, and overall system reliability.

This staged methodology ensured quantitative consistency between HIL emulation and physical testing, improving validation efficiency and safety.

V. REQUIREMENTS

Several parameters were updated from the project's initial phase to reflect practical insights gained during development.

The motor used is a custom-built, three-phase AC Induction Motor (ACIM) with 4 poles. Final specifications include:

- **Rated power:** 11 kW (peak 28 kW)
- **Rated torque:** 34.85 Nm (peak 94 Nm)
- **Rated speed:** 3000 RPM (max. 6000 RPM)
- **AC voltage (phase-to-phase):** 102 V
- **Max efficiency:** 86.6% at nominal load, PF = 0.54

The accumulator has a nominal voltage of 144 V and peaks near 164 V. The inverter voltage limit was set to 200 V to ensure margin and component reliability.

Inverter components were sized based on motor power, estimated losses, and safety margins, resulting in a max input power of 40 kW.

Ambient temperature was set at 40°C, based on past competition conditions.

The motor's maximum electrical frequency, at 6000 RPM, is calculated using (1) to be 200 Hz. Considering slip (s), typical in ACIMs, the actual frequency is slightly higher, as given by (2), aligning with the datasheet's 206 Hz.

$$f_{sync} = \frac{RPM \times Poles}{120} \tag{1}$$

$$f_{actual} = f_{sync} \times (1 + s) \tag{2}$$

A PWM frequency of 10 kHz was selected, striking a balance between minimizing current ripple and reducing switching losses. Being over a decade higher than the motor's electrical frequency, it also provides ample resolution for accurate control. Additionally, 10 kHz is a widely adopted standard, while lower frequencies may cause audible noise.

The final external requirements are summarized in Table I.

TABLE I. Finalized Project Requirements

Parameter	Value
High-Voltage System Voltage	144 V nominal (max. 200 V)
Motor Rated Power	11 kW (peak 28 kW)
Inverter Peak Input Power	40 kW (including safety margin)
PWM Frequency	10 kHz
Switching Technology	IGBTs (Silicon)
Low-Voltage System Voltage	12 V
Ambient Temperature	40°C
Maximum Motor Efficiency	86%

VI. DEVELOPMENT

This section presents the design rationale, implementation, and validation considerations for the developed voltage-source inverter. Rather than merely documenting hardware construction, the following subsections analyze the design decisions that most influenced performance, reliability, and control accuracy. Each subsystem, ranging from sensing and isolation to the power stage and gate driving, was developed with a focus on experimental validation and quantitative correlation with simulation and hardware-in-the-loop (HIL) results.

A. Block Diagram of Sensorless Field-Oriented Control Application

Fig.2 presents the block diagram of the sensorless field-oriented control application based on the previously discussed architecture. The code is distributed between user memory (FLASH/RAM), shown in green, and read-only memory (ROM), shown in orange [14].

The main components shown in the diagram are summarized below:

- **TMS320F28069M Microcontroller:** Acts as the central processing unit, executing control algorithms and managing system components.
- **InstaSPIN Library:** Stored in ROM, it contains the FAST (Flux, Angle, Torque, Speed) estimator, which enables accurate sensorless rotor angle tracking using real-time phase current, phase voltage, and DC-link voltage measurements.
- **PI Controllers:** Two PI controllers regulate the Id (magnetizing) and Iq (torque-producing) current components to achieve control targets.
- **Clarke, Park, and Inverse Park Transforms:** Perform transformations between three-phase and DQ reference frames, enabling vector-based control of the motor.
- **Speed PI Controller:** Regulates motor speed when torque references are not directly provided, adjusting the speed command as necessary.
- **SVM (Space Vector Modulation):** Generates PWM signals based on DQ-frame voltages to drive the motor.
- **HAL_run and HAL_readAdcData:** HAL_run updates PWM outputs, while HAL_readAdcData reads ADC values after conversion interrupts.

For a deeper understanding of the system's operation, it is beneficial to present the equations related to the PI controllers and the Clarke and Park transformations. The PI controllers for the d- and q-axis currents are shown in (3) and (4), respectively, while the speed control loop is described by (5). The Clarke and Park transformations, which map three-phase currents to the α–β and d–q reference frames, are defined in (6) and (7).

$$V_d = K_{p\_Id} \cdot (I_{d\_ref} - I_d) + K_{i\_Id} \cdot \int (I_{d\_ref} - I_d)dt \quad (3)$$

$$V_q = K_{p\_Iq} \cdot (I_{q\_ref} - I_q) + K_{i\_Iq} \cdot \int (I_{q\_ref} - I_q)dt \quad (4)$$

$$Spd_{\text{out}} = K_{p_{\text{speed}}} \cdot (\omega_{ref} - \widetilde{\omega}) + K_{i_{\text{speed}}} \cdot \int (\omega_{ref} - \widetilde{\omega})dt \quad (5)$$

$$\begin{bmatrix} I_\alpha \\ I_\beta \end{bmatrix} = \frac{2}{3} \begin{bmatrix} 1 & -\frac{1}{2} & -\frac{1}{2} \\ 0 & \frac{\sqrt{3}}{2} & -\frac{\sqrt{3}}{2} \end{bmatrix} \begin{bmatrix} I_a \\ I_b \\ I_c \end{bmatrix} \quad (6)$$

$$\begin{bmatrix} I_d \\ I_q \end{bmatrix} = \begin{bmatrix} \cos(\theta) & \sin(\theta) \\ -\sin(\theta) & \cos(\theta) \end{bmatrix} \cdot \begin{bmatrix} I_\alpha \\ I_\beta \end{bmatrix} \quad (7)$$

This block diagram encapsulates the foundational structure of the sensorless field-oriented control application, enabling precise and efficient motor control, with the added capability of speed control in driverless mode (when torque references are not directly provided).

B. Isolation

Electrical isolation between the high-voltage (HV) and low-voltage (LV) domains is essential for operator safety and reliable system operation, as required by Formula SAE Electric regulations. The inverter integrates reinforced galvanic isolation through UL 1577–recognized gate drivers powered by dedicated isolated DC/DC converters with withstand voltages above 3 kV. Critical feedback signals from the HV side are transferred via isolated amplifiers (AMC1411), compliant with DIN VDE V 0884-11:2017-01, ensuring accurate and safe signal transmission.

All external communication, including the vehicle's Controller Area Network (CAN), is also galvanically isolated to prevent ground loops and ensure system integrity during transients. This comprehensive isolation strategy meets automotive safety standards while maintaining signal fidelity and noise immunity across all interfaces.

C. Voltage Sensing

Accurate voltage measurement is essential for reliable inverter control and protection. The three phase voltages and the DC-link voltage are measured through galvanically isolated channels using the Texas Instruments AMC1411 amplifier. Each sensing path includes a first-order low-pass filter with a 243 Hz cutoff, attenuating switching noise while preserving the fundamental components required for control.

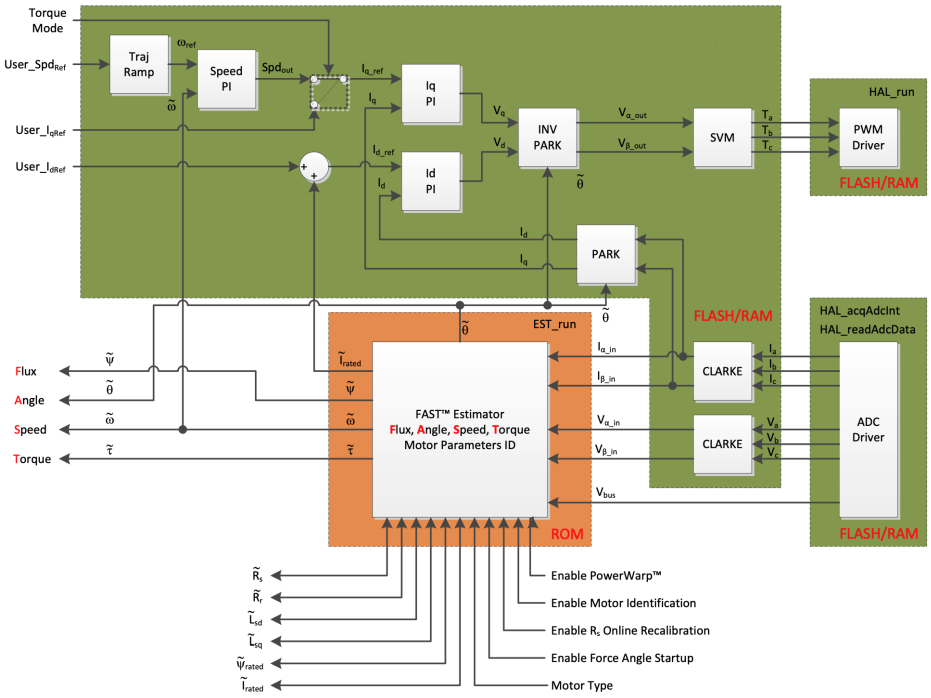

FIGURE 2. Block Diagram of the Sensorless Field-Oriented Control Application

Resistive dividers scale the signals to the AMC1411 input range of 0–2 V, and a secondary operational amplifier converts the differential output to a single-ended signal within the 0–3.3 V range for the TMS320F28069M microcontroller. This configuration ensures accurate, isolated, and low-noise voltage feedback for both control and diagnostic functions.

D. Current Sensing

Accurate current feedback is essential for precise torque control in field-oriented control (FOC) operation. Each motor phase current is measured using a LEM HO 150-S-0100 open-loop Hall-effect transducer, rated for 150 ARMS with 1 % typical accuracy and powered from a single 5 V supply.

The sensor output is buffered by a unity-gain operational amplifier to preserve signal integrity and drive the ADC input. A resistive divider combined with a first-order low-pass filter scales the 0–5 V signal to the 0–3.3 V range required by the TMS320F28069M microcontroller, with a 1 kHz cutoff to suppress switching noise. This compact conditioning stage provides low-latency, low-noise current feedback suitable for real-time motor control and protection.

E. IGBT Selection

Three FF400R12KE3 dual IGBT modules were selected for this project due to their robust electrical and mechanical characteristics. Their screw terminals ensure reliable high-current connections with copper bars or cables, reducing the risk of damage to the control board, as illustrated in Fig.3. The main specifications of the module are summarized in TableII.

TABLE II. FF400R12KE3 IGBT Module Specifications

Specification	Value
Voltage Rating	1200 V
Current Rating	400 A per module
Configuration	Dual IGBT
Mounting Type	Screw Terminals
Dimensions	150 mm × 62 mm × 17 mm
Weight	0.42 kg per module

Although the modules exceed the system's current requirements, their selection, made possible through collaboration with a partner company, provides operational headroom and facilitates future upgrades without necessitating hardware changes.

FIGURE 3. IGBT Modules, DC-Link capacitor and cold plate

F. Gate Driver Selection

The inverter system operates with isolated voltage sources to power each of the six transistors. Each transistor is equipped with a dedicated isolated gate driver, specifically the Infineon 1ED3491MC12M (CLAMPDRV variant) [15]. This gate driver enables isolated control between the low-voltage (LV) and high-voltage (HV) sides and includes integrated protection functions essential for IGBT safety and system reliability. Each channel is supplied by an isolated DC/DC converter providing $+15\,\mathrm{V}/-9\,\mathrm{V}$.

Operational principles (with selected parameters).

- **Desaturation (DESAT) short-circuit protection**: monitors the collector–emitter voltage through a high-voltage diode and series resistor into the DESAT pin. If the sensed V_{CE} exceeds the internal threshold after the leading-edge blanking interval and within the digital filter window, the driver latches a fault and initiates a controlled soft turn-off.
  Selected values: t_{LEB} =650 ns; t_{FIL} =1775 ns; R_{DESAT} =1 kΩ; DESAT diode = MMSD301T1G;
- **Active soft turn-off**: upon DESAT, a programmable current source discharges the gate to limit di/dt.
- **Active Miller clamp (CLAMPDRV)**: an external small-signal nMOS, driven by the CLAMP output and placed close to the gate–emitter Kelvin pair, sinks Miller current during turn-off to avoid spurious turn-on of the complementary device under high dv/dt. *Selected values:* clamp MOSFET = NTGS3136PT1G; $R_{\mathrm{G,on}}$ =4.2 Ω.
- **Undervoltage lockout (UVLO)**: operation is permitted only when the output-side supply satisfies $V_{\mathrm{CC2}} - V_{\mathrm{EE2}} > V_{\mathrm{UVLO,TH}}$, preventing linear-region drive and excess losses.

G. DC-Link Capacitor Selection

The DC-link capacitor plays a critical role in stabilizing the inverter's intermediate bus voltage and limiting current ripple, which directly affects switching losses and electromagnetic interference. The current ripple magnitude depends on the motor phase inductance, switching frequency, and DC-link voltage, as expressed in (8), while the resulting voltage ripple can be estimated from (9) [16].

$$\Delta i = \frac{0.5 \cdot V_{bus}}{f \cdot L} \tag{8}$$

$$\Delta v = \frac{V_{bus}}{32 \cdot L \cdot C \cdot f^2} \tag{9}$$

Based on these relationships, the EPCOS B25631A0187K800 film capacitor was selected for its high capacitance, low equivalent series resistance (ESR), and current-handling capability, ensuring minimal voltage ripple and thermal stress under the inverter's rated operating conditions.

H. Data Acquisition System

To facilitate comprehensive data collection during testing and competition, the team developed a secondary telemetry system. The vehicle architecture includes two independent CAN networks: one for the low-voltage (LV) system and another for the tractive system (TS) components such as the Battery Management System (BMS) and the inverter, with the main ECU bridging between them.

The developed telemetry system is based on a T-CAN485 board featuring an ESP32 microcontroller, a CAN transceiver, and a microSD card interface. This system enables the capture and storage of CAN messages for subsequent offline analysis.

Additionally, leveraging the ESP32's built-in Wi-Fi and Bluetooth capabilities, a wireless parameterization system was implemented. It allows adjustments to key inverter parameters, such as the current controller's Iq reference multipliers, enhancing tuning flexibility. To streamline the debugging and testing process further, a mobile application was developed, providing real-time wireless visualization of critical system data.

I. Cooling System

The cooling system was designed to be simple and low-cost, aligning with the project's resource constraints. To estimate the thermal losses of the power semiconductors, thermal simulations were performed using **Infineon's IPOSIM tool** under the nominal operating conditions summarized in Table III. Based on these simulations, the **estimated losses were 80.20 W per IGBT and 32.50 W per diode**.

TABLE III. Thermal Simulation Conditions

Parameter	Value
Modulation algorithm	SVPWM
DC-link voltage V_{DC}	144 V
Output current I_{out}	133 A_{rms}
Output frequency	103 Hz
Switching frequency	10 kHz
Cold plate temperature	40 °C

An important consideration during the design phase was an initial interpretation in which these per-device loss values were considered total losses per module. However, due to unrelated vehicle issues encountered during the competition, the inverter was not subjected to continuous full-capacity thermal stress; thus, this initial interpretation regarding loss distribution did not ultimately impact the observed operational performance in the vehicle.

It is also important to note that the Endurance event does not operate under constant nominal conditions. Power levels are generally lower and vary significantly over time, resulting in substantially lower average losses compared to those simulated for worst-case scenarios.

To validate the thermal solution in a controlled environment, a reused radiator was experimentally tested using

a submerged resistive heater adjusted to match the total estimated worst-case power loss of approximately 650 W. During this test, the system reached a stable temperature of 47 °C within 17 minutes at an ambient temperature of 27 °C. This experimental result confirms the radiator's capacity to dissipate the applied load, thereby validating the adequacy of the cooling system's theoretical design and components for the expected thermal demands during competition, even though a full-scale thermal validation on the vehicle itself was not achieved.

J. PCB Design and Manufacturing

The Control and Driver Boards were designed as four-layer printed circuit boards (PCBs) to balance electrical performance, cost, and manufacturability. The outer layers use 1 oz copper for power and signal routing, while the inner layers employ 0.5 oz copper—one dedicated as a continuous ground plane to enhance electromagnetic compatibility and signal integrity, and the other as a low-voltage supply plane.

High-voltage areas maintain a minimum clearance of 3 mm in accordance with FSAE electrical safety regulations and are protected with a conformal coating to improve insulation reliability under environmental stress. Fast-switching traces are routed on the top layer and low-speed signals on the bottom to minimize coupling between noisy and sensitive nets. This layout approach provides a compact, EMC-robust, and safety-compliant foundation for the inverter electronics.

VII. HARDWARE ASSEMBLY

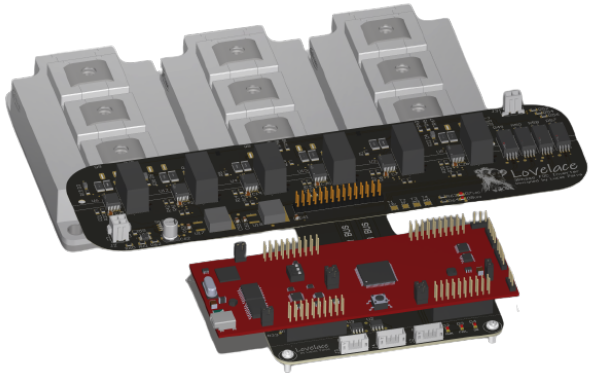

FIGURE 4. Comprehensive overview of the inverter hardware assembly.

This section presents an overview of the inverter system's hardware assembly, highlighting the modular and adaptable structure developed to support future enhancements.

To provide a clear understanding of the system architecture, two key visual aids are included. Fig. 5 presents a block diagram outlining the main functional units and their interconnections, covering both power and control signal paths. Complementarily, Fig. 4 offers a top-level view of the physical arrangement and modular integration of the Printed Circuit Boards (PCBs).

A. Developed Structure

A core design principle of this project is modularity. To facilitate testing, upgrades, and maintenance, the hardware was divided across multiple dedicated PCBs. This modular approach is illustrated in the block diagram shown in Fig. 5.

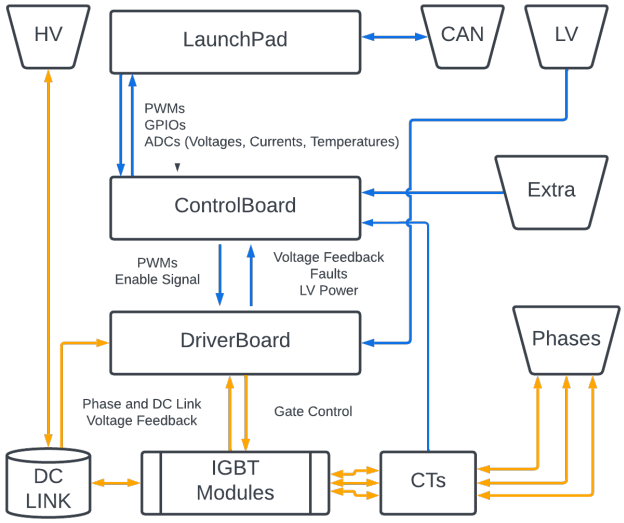

FIGURE 5. Block diagram of the inverter system, highlighting modular components.

The diagram uses color coding to distinguish between low-voltage (LV) and high-voltage (HV) sections. Key components include the LaunchPad microcontroller, the custom ControlBoard and DriverBoard PCBs, and the current transformers (CTs). Trapezoidal shapes mark the primary interfaces: the high-voltage power input from the accumulator, the low-voltage 12 V supply, CAN communication with the vehicle's network, motor terminals for three-phase bidirectional current, and reserved connectors for future system expansion.

This modular design improves development efficiency, enhances fault isolation, and increases the system's flexibility for future iterations.

B. Control Board

The Control Board is a custom-designed PCB that manages essential functions within the inverter system. A LAUNCHXL-F28069M development board was selected to host the TMS320F28069M microcontroller, offering greater flexibility compared to a standalone configuration. This board integrates an XDS100v2 JTAG debugger and an onboard 3.3 V CAN transceiver (Texas Instruments SN65HVD234D), as shown in Fig. 6. The CAN bus is connected directly to the LaunchPad's transceiver, eliminating the need for an additional external CAN interface.

Designed to interface with the LaunchPad, the Control Board primarily conditions feedback signals for the microcontroller. It processes differential voltage feedback signals

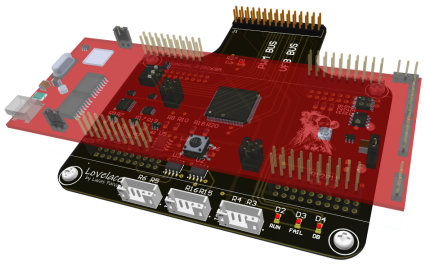

FIGURE 6. Control Board

from the three phases and the DC bus, and adapts the current transformer outputs through buffering and filtering.

In addition to signal conditioning, the Control Board integrates LEDs for debugging, connections for temperature sensors, and handles fault and low-voltage feedback signals. It receives power from the Driver Board and routes all signals through a shared bus.

Furthermore, the Control Board implements hardware protection features using the LM339 comparator. Each of the three current transducer signals is monitored for both positive and negative current limits, enabling phase overcurrent detection. The DC-link voltage is also monitored for both undervoltage and overvoltage conditions. If any of these conditions are detected, the comparator outputs can trigger a soft shutdown of the IGBTs through the gate driver, helping to protect the system against potentially damaging electrical faults.

C. Driver Board

The Driver Board is a crucial component responsible for controlling the IGBT modules. It's positioned directly above these modules, as shown in Fig. 7. Each IGBT is precisely controlled by an isolated gate driver, which has its isolated DC/DC converter, delivering +15/-9 V.

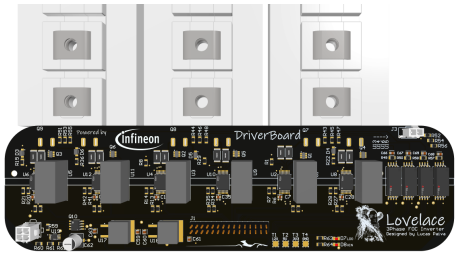

FIGURE 7. Driver Board

This board plays a pivotal role in gathering the four essential voltage measurements required for the system. While phase voltages are captured through dedicated connectors in the IGBT modules, the DC bus voltage measurement necessitates an external connection due to unexposed collector pins in high-side transistors. The board also handles LV supply, performing functions such as protection against voltage conditions, and then distributes 12 V to the gate driver's DC/DC converters. Additionally, two Low Drop-Out (LDO) voltage regulators produce stable 5 V and 3.3 V outputs for powering logic components, including the microcontroller.

To further enhance robustness, the Driver Board integrates an LTC4367 Overvoltage, Undervoltage, and Reverse Supply Protection Controller on the low-voltage input. This device safeguards the system against supply faults such as overvoltage, undervoltage, reverse polarity, and inrush current, ensuring safe startup and reliable operation under harsh electrical conditions.

VIII. SYSTEM VALIDATION: HARDAWARE-IN-THE-LOOP (HIL)

To validate the initial development of the inverter control system, a Hardware-in-the-Loop (HIL) platform was extensively used, providing a safe and efficient environment to test control algorithms, motor dynamics, and CAN-based communication strategies before real-world integration. A custom HIL model was created using the actual motor parameters and a battery model replicating the electrical characteristics of the vehicle's accumulator pack. An overview of the HIL setup is shown in Fig. 8.

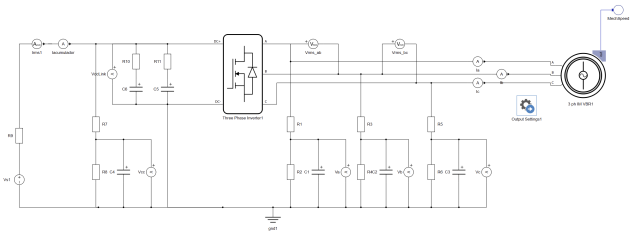

FIGURE 8. Schematic Diagram of the HIL Setup

The HIL platform initially supported validation of the motor control behavior, focusing on the interaction between the current PI controllers and the speed controller used during autonomous operation. A dynamic load model was then introduced to emulate varying mechanical loads and assess system acceleration and torque response, followed by validation of regenerative braking functionalities to ensure proper energy feedback management.

Additionally, the HIL system was crucial for verifying the robustness of CAN-based telemetry and control under extreme conditions, and for safely implementing software-based overcurrent protection strategies. Physical bench testing was limited by available equipment, restricting achievable power levels to a small fraction of the inverter's capacity, making HIL simulation an indispensable tool for comprehensive system validation prior to vehicle integration.

IX. INITIAL BENCH VALIDATION

Fig. 9 shows the initial hardware validation setup, assembled outside of its final enclosure. This approach facilitated easier access to measurement points and ensured broad ventilation during the early testing phases.

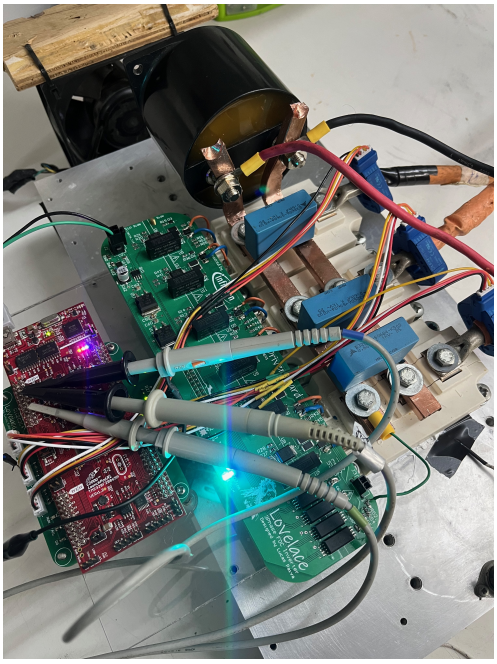

FIGURE 9. Initial Bench Validation

Each printed circuit board (PCB) was individually tested prior to full system integration, allowing for early identification of hardware issues and simplifying troubleshooting.

Initial tests of the DSP-controlled system were conducted in open-loop mode, enabling basic functionality checks without the complexities of closed-loop control. During this phase, electromagnetic interference (EMI) affecting the current sensors was identified and mitigated by replacing and shielding the signal cables.

As closed-loop operation was introduced, ensuring the integrity of feedback signals became critical due to the sensorless control strategy. To improve signal quality, the capacitors in the low-pass filters of the phase voltage sensors were replaced, reducing the cutoff frequency to attenuate high-frequency harmonics from switching activity.

Load testing was then performed within the limitations of the available DC power supply, which delivered approximately 10 kW (see Section VIII). A secondary motor, rated at 5 kVA and compatible in speed, was mechanically coupled to the test motor via a custom 3D-printed adapter. Its terminals were connected to a resistive load bank to dissipate the generated energy.

Under these conditions, key measurements were taken, including the line voltage between phases B and C and the phase B current, at 155 V DC bus voltage, 40 A DC input current, and 2100 RPM motor speed (see Fig. 10). To better represent signal behavior, the acquired oscilloscope data was post-processed using first-order low-pass filters with cutoff frequencies of approximately 243 Hz for voltage and 1 kHz for current. These match the analog filters used in hardware prior to ADC acquisition.

Although full nominal power testing was not possible, the series of tests, including individual PCB validation, successful EMI mitigation, and stable closed-loop operation under load, confirmed the inverter's fundamental operational integrity. The observed stable waveforms and expected control responses under these conditions provided critical confidence for proceeding with vehicle-level integration, demonstrating its readiness for initial on-vehicle trials within the Formula Student environment.

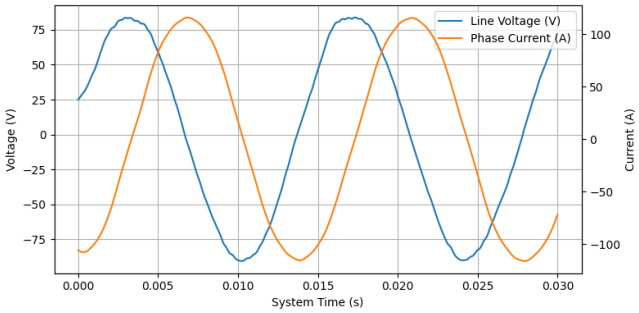

FIGURE 10. Line voltage between phases B and C and phase B current

X. VEHICLE SHAKEDOWN

Following initial bench validations, the inverter system was integrated into the Formula Student vehicle for further testing and refinement.

During the 2024 season, the team encountered significant reliability issues with the accumulator. Due to delays and safety considerations, it was decided to limit the maximum extracted power to approximately 10–15 kW. Although this reduced the vehicle's peak performance, it prioritized system integrity and operational safety.

To enable integration with the vehicle chassis, a custom enclosure for the inverter was fabricated using 3D-printed PETG filament with flame-retardant properties.

In the initial shakedown configuration, the speed controller was disabled, and the Iq current controller received direct input from the accelerator pedal. However, the speed controller was preserved for autonomous operation, where a secondary onboard computer would provide the speed reference.

Control commands and operational modes were transmitted from the main ECU to the inverter via the tractive system CAN network at 40 Hz, with telemetry data sent back at the same rate.

Throughout this phase, temperature monitoring and fine-tuning of the control loops were critical. A hardware issue was encountered involving the failure of a thermistor monitoring the cold plate temperature, which resulted in a short circuit that damaged the DSP. The fault caused excessive

current draw, leading to overheating and shutdown of the 5 V regulation system due to LDO thermal protection.

Corrective actions involved replacing both the damaged DSP and thermistor, along with implementing an additional protection circuit to prevent similar failures in future operations.

XI. REAL-WORLD PERFORMANCE AND VALIDATION

The final stages of validation involved evaluating the inverter system's performance under actual dynamic and competitive conditions. This section presents results from the Formula SAE Brazil 2024 competition and, crucially, enhanced validation data obtained from recent testing of the 2025 Formula Student Electric vehicle, which integrates an updated inverter design (featuring similar technical and thermal characteristics, with improvements primarily in enclosure material and busbar layout).

A. Formula SAE Brazil 2024 Competition Results

During the Formula SAE Brazil 2024 competition, the vehicle equipped with the initially developed inverter system was taken to the track. Thanks to the project's detailed documentation and rigorous preparation, the inverter system successfully passed the competition's mandatory electrical inspection without issues. However, unrelated problems within other subsystems of the vehicle caused delays in completing both electrical and mechanical inspections. As a result, the team was only able to participate in the final dynamic event, the Endurance race.

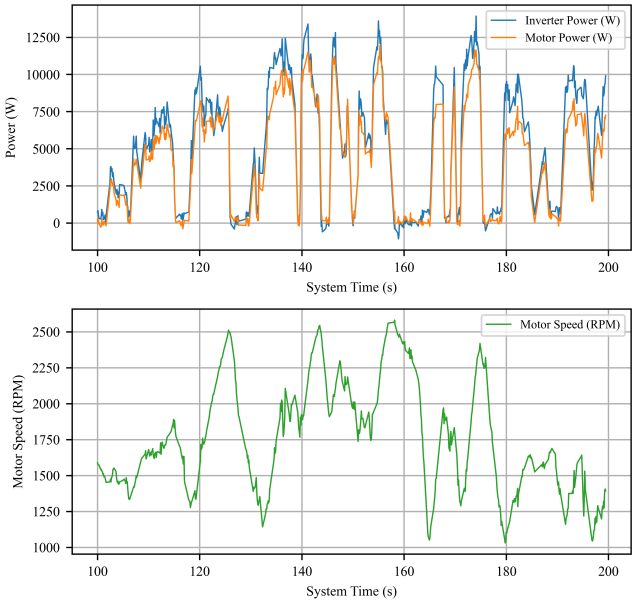

FIGURE 11. Enduro Data (Formula SAE Brazil 2024)

As shown in Fig. 11, the vehicle completed *4* laps, consuming a total of *0.638* kWh. This performance established a new endurance record for the team and demonstrated the inverter's reliability and energy efficiency under real competition conditions. Nevertheless, due to extremely high ambient temperatures on the day of the event, the vehicle's monitoring systems detected excessive temperature levels, leading to a strategic decision to disable the tractive system to preserve hardware integrity. While the inverter's fundamental operation was sound, this experience highlighted areas for improved thermal management at the vehicle system level in future designs.

In the static events, the results were even more positive. The Design Event, in particular, yielded outstanding outcomes. Within the powertrain category, which included the inverter system, the team achieved the highest score among all competitors. This strong performance in the powertrain area contributed significantly to the team's overall success, culminating in a first-place finish in the Design Event.

B. Enhanced On-Vehicle Validation with 2025 Prototype

Building upon the experiences and lessons from the 2024 competition, further comprehensive on-vehicle testing was conducted with the 2025 Formula Student Electric prototype. This prototype employs a refined version of the developed inverter, retaining its core technical characteristics while introducing key improvements in the enclosure, cold plate assembly—aimed at enhancing thermal performance—and busbar design for increased mechanical robustness. These upgrades enabled more effective thermal management and structural resilience under demanding conditions. The tests facilitated controlled data acquisition during dynamic driving scenarios, offering deeper insights into the inverter's electrical performance and thermal behavior in realistic operating environments.

During representative acceleration runs, the inverter demonstrated excellent dynamic response and control fidelity. As illustrated in Fig. 12, it closely tracked torque and power demands during high-load transitions, enabling rapid acceleration from 0 to 50 km/h in 2.7 seconds. In addition to strong motoring performance, the system also exhibited effective energy recovery, reaching a peak of 5 kW during regenerative braking phases. These results confirm the inverter's capability to deliver precise torque control, stable power output, and efficient bidirectional energy flow under dynamic load conditions.

Unlike the 2024 competition season, where the inverter's output was intentionally limited to approximately 10–15 kW due to accumulator constraints, the 2025 prototype operated with reduced power limitations and achieved a measured peak power of approximately 17 kW. This demonstrates the system's enhanced capability under representative operating conditions.

Fig. 13 shows the inverter's thermal behavior during a sequence of repeated acceleration events, recorded under an ambient temperature of **16 °C**. Despite the high power demand , the inverter's internal temperature remained well within safe limits, peaking at just **24.3 °C**, indicating effective thermal management.

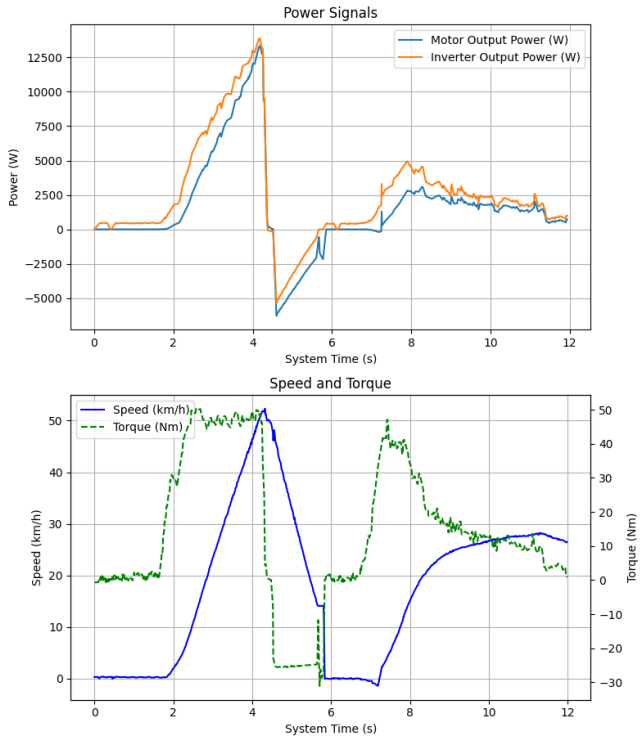

FIGURE 12. Inverter Performance during Acceleration Event (2025 Prototype): Power Output, Vehicle Speed, and Motor Torque.

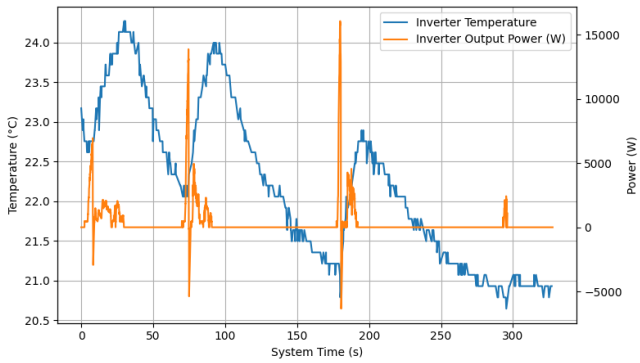

FIGURE 13. Inverter Temperature Evolution Across 3 Acceleration Events (2025 Prototype).

For extended operational validation, the 2025 prototype successfully completed a total of **18.5 km** of on-track testing, encompassing various driving cycles and sustained load scenarios. Throughout these trials, the inverter's temperature was continuously monitored, with a peak internal value of **35 °C**, recorded under an ambient temperature of **20°C**. This confirms the inverter's robust thermal design and its suitability for prolonged high-performance operation in a Formula Student context.

To consolidate the key performance metrics obtained during on-vehicle testing, Table IV summarizes the main quantitative results.

TABLE IV. Summary of Measured Performance During Vehicle Testing

Metric	Measured Value
0–50 km/h acceleration	2.7 s
Peak power	17 kW
Peak regenerative power	5 kW
Inverter internal temperature (ambient 20 °C)	35.0 °C (peak)
Total on-track testing distance	18.5 km
Energy used during endurance event (4 laps)	0.638 kWh

XII. CONCLUSION

This work presented the development, validation, and real-world application of a three-phase voltage source inverter using field-oriented control (FOC) and space vector modulation (SVM) for a Formula Student electric vehicle.

The inverter was initially validated through Hardware-in-the-Loop (HIL) simulations and bench testing, ensuring the effectiveness of control strategies, protection systems, and telemetry before deployment. HIL played a crucial role in refining the control software despite bench testing limitations.

Following successful validations, the inverter was integrated into the team's vehicle and performed reliably during the 2024 Formula SAE Brazil competition, passing technical inspections and contributing to a new endurance performance record. It also helped secure the highest powertrain score, a first-place finish in the Design Event, and an overall second-place result for the team.

APPENDIX

A. Gate Driver and Isolated Supply

Figure 14 presents the schematic of a single gate-driver channel, representative of the six identical phases implemented in the inverter.

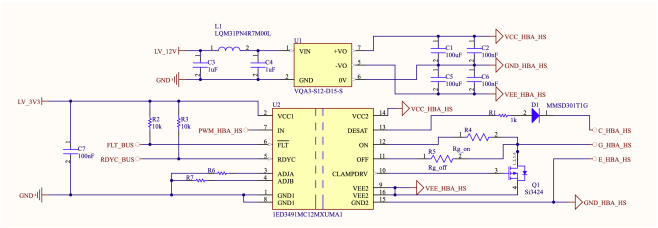

FIGURE 14. Schematic of one isolated gate-driver channel.

B. Voltage Sensing Circuits

Accurate measurement of both DC-link and phase voltages is achieved through isolated amplifier stages. The sensing chain is divided into two functional parts:

- **Isolated differential amplifier:** the AMC1411 receives the scaled voltage from a precision divider, with a first

order filter, and transfers it across the isolation barrier. (Fig. 15).

- **Differential-to-single-ended:** on the controller side, the differential signal is converted to single-ended. (Fig. 16).

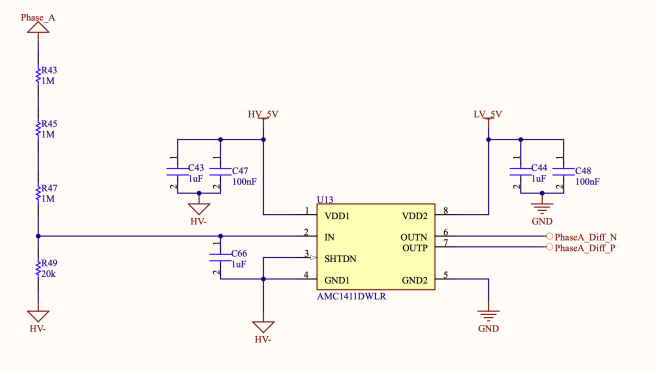

FIGURE 15. Voltage sensing input stage. Capacitor C66 value was adjusted in the assembled hardware to match the target filter bandwidth.

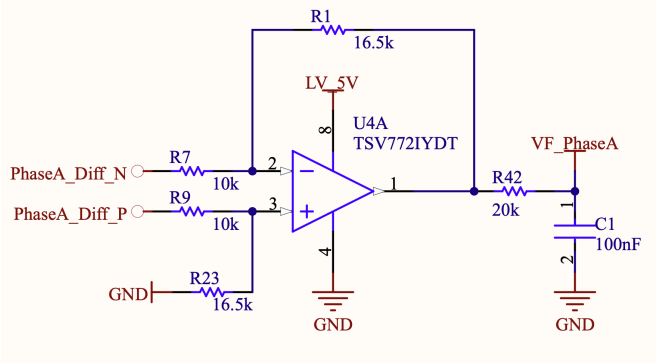

FIGURE 16. Post-isolation differential-to-single-ended stage. Capacitor C1 not populated in the final hardware.

ACKNOWLEDGMENT

The authors would like to thank the Formula Student Electric teams for providing valuable reference materials that guided the project development [3], [4], [17].

Special thanks are due to Infineon Technologies for supplying critical components, to Typhoon HIL for providing the Hardware-in-the-Loop (HIL) equipment and technical support essential for the validation phase, and to Hercules Motores Elétricos for providing the electric motor used in the vehicle.

The authors also acknowledge the support from Ampera Racing, the Institute of Power Electronics (INEP), and Labmetro of the Federal University of Santa Catarina (UFSC), whose contributions were fundamental to the realization of this work.

REFERENCES

[1] L. P. Da Silva, G. Waltrich, "Driving Technological Advancements in Formula Student: Developing a Field-Oriented Control Voltage Source Inverter for Enhanced Motor Control", *in 2023 IEEE 8th Southern Power Electronics Conference and 17th Brazilian Power Electronics Conference (SPEC/COBEP)*, pp. 1–8, 2023, doi:10.1109/SPEC56436.2023.10407881.

[2] T. Moldovan, R. Inţe, R.-O. Nemeş, M. Ruba, C. Marţiş, "Typhoon HIL Real-Time Validation of Permanent Magnet Synchronous Motor's Control", *in 2021 9th International Conference on Modern Power Systems (MPS)*, pp. 1–6, Cluj-Napoca, Romania, 2021, doi:10.1109/MPS52805.2021.9492619.

[3] Wisconsin Racing Formula SAE Team, "120 kW Quad Inverter Report", https://www.wisconsinracing.org/wp-content/uploads/2020/10/WR_Quad_Inverter.pdf, accessed 2025-10-12, 2020.

[4] F. Stella, G. Pellegrino, E. Armando, "Three-phase Inverter for Formula SAE Electric with Online Junction Temperature Estimation of all SiC MOSFETs", *in Proc. IEEE Applied Power Electronics Conference and Exposition (APEC)*, pp. 1154–1161, 2020, doi:10.1109/APEC39645.2020.9124302.

[5] C. Zhang, S. Srdic, S. Lukic, Y. Kang, E. Choi, E. Tafti, "A SiC-Based 100 kW High-Power-Density (34 kW/L) Electric Vehicle Traction Inverter", *in Proc. IEEE Energy Conversion Congress and Exposition (ECCE)*, Portland, OR, USA, 2018, iSBN: 978-1-4799-7312-5.

[6] G.-j. Su, J. P. Wilkins, L. Xue, B. Ozpineci, R. Sahu, E. Gurpinar, "A High-Power Density Segmented Traction Drive Inverter", *in Proc. 2023 IEEE Energy Conversion Congress and Expo (ECCE)*, pp. 1825–1830, Nashville, TN, USA, 2023.

[7] B. Wrzecionko, D. Bortis, J. W. Kolar, "A 120 °C Ambient Temperature Forced Air-Cooled Normally-off SiC JFET Automotive Inverter System", *IEEE Transactions on Power Electronics*, vol. 29, no. 5, pp. 2345–2358, May 2014, doi:10.1109/TPEL.2013.2294906.

[8] F. Blaschke, "The Principle of Field Orientation as Applied to the New Transvector Closed-Loop Control System for Rotating-Field Machines", *Siemens Review*, vol. 39, no. 5, pp. 217–220, 1972.

[9] K. Zhou, D. Wang, "Relationship Between Space-Vector Modulation and Three-Phase Carrier-Based PWM: A Comprehensive Analysis", *IEEE Transactions on Industrial Electronics*, vol. 49, no. 1, pp. 186–196, Feb 2002, doi:10.1109/41.982262.

[10] F. Mihalič, M. Truntič, A. Hren, "Hardware-in-the-Loop Simulations: A Historical Overview of Engineering Challenges", *Electronics*, vol. 11, no. 15, p. 2462, 2022, doi:10.3390/electronics11152462, URL: https://www.mdpi.com/2079-9292/11/15/2462.

[11] W. Leonhard, *Control of Electrical Drives*, 3rd ed., Springer, Berlin, Heidelberg, 2001.

[12] J. Holtz, "Pulsewidth Modulation for Electronic Power Conversion", *Proceedings of the IEEE*, vol. 82, no. 8, pp. 1194–1214, 1994, doi:10.1109/5.301684.

[13] J. Uralde, O. Barambones, E. Artetxe, I. Calvo, A. del Rio, "Model Predictive Control Design and Hardware in the Loop Validation for an Electric Vehicle Powertrain Based on Induction Motors", *Electronics*, vol. 12, no. 21, p. 4516, 2023, doi:10.3390/electronics12214516, URL: https://www.mdpi.com/2079-9292/12/21/4516.

[14] Texas Instruments, *InstaSPIN-FOC™ and InstaSPIN-MOTION™ User's Guide (Rev. 1)*, 2021.

[15] Infineon Technologies, *EiceDRIVER™ 1ED34x1Mc12M Enhanced: Single-channel isolated gate driver IC with adjustable DESAT and soft-off*, 2021, URL: https://www.infineon.com/dgdl/Infineon-1ED34x1Mx12M-DataSheet-v01_10-EN.pdf, datasheet v2.1.

[16] M. Salcone, J. Bond, "Selecting Film Bus Link Capacitors for High Performance Inverter Applications", *in 2009 IEEE International Electric Machines and Drives Conference*, pp. 1692–1699, Miami, FL, USA, 2009, doi:10.1109/IEMDC.2009.5075431.

[17] C. Markgraf, L. Gacy, S. Leitenmaier, D. Lengerer, B. Schwartz, D. W. Gao, "Autonomous Electric Race Car Inverter Development: Revving up the Future with Resource Efficient Drive Technology", *IEEE Electrification Magazine*, vol. 11, no. 2, pp. 52–61, June 2023, doi:10.1109/MELE.2023.3264921.

AUTHOR'S CONTRIBUTIONS

L.P.SILVA: Conceptualization, Data Curation, Formal Analysis, Funding Acquisition, Investigation, Methodology, Project Administration, Resources, Software, Validation, Visualization, Writing – Original Draft, Writing – Re-

view & Editing. **G.WALTRICK:** Formal Analysis, Funding Acquisition, Project Administration, Resources, Supervision, Validation, Visualization, Writing – Review & Editing. **D.J.REGNER:** Funding Acquisition, Resources, Software, Visualization. **T.L.F.COSTA:** Funding Acquisition, Resources, Software, Visualization.

PLAGIARISM POLICY

This article was submitted to the similarity system provided by Crossref and powered by iThenticate – Similarity Check.

DATA AVAILABILITY

The data used in this research is available in the body of the document.

BIOGRAPHIES

Lucas Paiva da Silva earned a technical qualification in Electronics from the Federal Institute of Santa Catarina (IFSC) in 2019 and is currently completing his B.Sc. degree in Electrical Engineering at the Federal University of Santa Catarina (UFSC), Brazil. He has worked with real-time simulation, embedded motor-control systems, and power-electronics converter development through research activities at the Institute of Power Electronics (INEP/UFSC) and an internship at Typhoon HIL, focusing on high-performance HIL models and custom toolchain development. From 2020 to 2025, he contributed to the Ampera Racing Formula SAE Electric team, where he led the design and experimental validation of a three-phase traction inverter for electric-vehicle applications. He is currently undertaking an Electronics & ERS Systems Student Placement at Red Bull Powertrains (RBPT) in Milton Keynes, working on hybrid power-unit technologies for Formula 1. His main interests include electric-vehicle propulsion systems, real-time HIL simulation, motor control, embedded systems and power electronics.

Gierri Waltrich received his B.Sc. (2007) and M.Sc. (2009) degrees in Electrical Engineering from the Federal University of Santa Catarina (UFSC), Brazil, and his Ph.D. degree (2013) in Electrical Engineering from the Eindhoven University of Technology, The Netherlands, specializing in power electronics. He is currently a Full Professor with the Department of Mechanical Engineering at UFSC, working with the Instrumentation and Automation Laboratory (LABMETRO) and the Institute of Power Electronics (INEP). He is also a permanent faculty member of UFSC's Graduate Program in Electrical Engineering (PPGEEL). His research interests include electric vehicles, multilevel converters, dc–dc, dc–ac and ac–ac power conversion, smart grids, and advanced measurement methods.

Daniel Juchem Regner received his B.Sc. degree in Control and Automation Engineering and his M.Sc. degree in Mechanical Engineering, with a focus on metrology and instrumentation, both from the Federal University of Santa Catarina (UFSC), Brazil. He has over five years of experience in petroleum pipeline inspection using aerial robots, having developed an automatic inspection system employed in his master's research. He is currently a researcher working primarily in computer vision.

Tiago Loureiro Figaro da Costa Pinto received his B.Sc. degree in Control and Automation Engineering from Universidade Paulista (1998), where he received two merit awards from CREA-SP and the Engineering Institute. He obtained his M.Sc. degree in Scientific and Industrial Metrology (2001) and his Ph.D. degree in Mechanical Engineering, with concentration in Metrology and Instrumentation (2010), both from the Federal University of Santa Catarina (UFSC), Brazil. He is currently an Associate Professor at the Department of Mechanical Engineering at UFSC. His research interests include scientific and industrial metrology, optical and dimensional metrology, coordinate metrology, measurement automation, mechatronic systems for inspection, robotics, RPAS (drones), and system integration.